

## **ANALYSIS OF CLUTTER REDUCTION TECHNIQUES FOR THROUGH WALL IMAGING IN UWB RANGE**

**P. K. Verma, A. N. Gaikwad, D. Singh, and M. J. Nigam**

Department of Electronics and Computer Engineering  
Indian Institute of Technology Roorkee  
Roorkee 247667, India

**Abstract**—Nowadays, through wall imaging (TWI) is an emerging topic of research in which one of the most important tasks is to minimize the clutter through which detection accuracy can be improved. Clutter in TWI is due to many reasons like wall coupling, antenna coupling, multiple reflections etc. To analyze the clutter reduction techniques, firstly we indigenously assembled a TWI system (i.e., step frequency continuous wave radar (SFCW)) in UWB range (freq. 3.95 GHz to 5.85 GHz), and different observations have been taken. We have considered metallic plate and one more material with low dielectric constant (Teflon) as a target and kept them behind the plywood wall. A-scan and B-scan observations have been carried out. The observed data are preprocessed for imaging and then different types of clutter reduction techniques like Principal Component Analysis (PCA), Independent Component Analysis (ICA), Factor Analysis (FA) and Singular Value Decomposition (SVD) have been applied, and results were analyzed. Signal to noise ratio (SNR) of the final images (i.e., after clutter removal with different techniques) has been computed to compare the results and know the effectiveness of individual clutter removal techniques. It is observed that ICA has better capability to remove the clutter in comparison to other applied techniques; especially it is found that ICA has a capability to distinguish the difference between clutter and low dielectric target whereas other clutter removal techniques are not showing significant result.

## 1. INTRODUCTION

Surveillance/navigation systems such as television, infrared, and other line-of-sight surveillance hardware are extensively used nowadays. However, these systems cannot tell what is happening or locate persons/assets on the other side of a wall, behind bushes, in the dark, in a tunnel or a cave, or through a dense fog. X-rays may be used for such purposes, but since they possess health risk, they are avoided. For an effective detection system, the radar should have a transmitted signal at a frequency low enough that should be capable of penetrating walls and have a very wide bandwidth so that targets behind walls may be clearly identified. Bandwidths need to be several gigahertz to achieve high resolution. UWB radar systems satisfy these low frequency and large bandwidth requirements; they are defined as those for which the relative bandwidth is equal to or greater than 20%.

Through wall detection [1–3] is an emerging field in research because of its application in human monitoring, disaster search and rescue, physical security, law enforcement, and urban military operations. In TWI system, the electromagnetic waves that are transmitted by the radar have to propagate through the air, non metallic wall and other objects. TWI radar has capability to detect any objects that lie in its line of sight if the conductivity of object or dielectric constant or permeability is different from the surrounding medium. It is usually the contrast in the permittivity that leads to a reflection of the electromagnetic waves radiated by the transmit antenna and helps in detection process. The reflected signal also depends on the ratio between the size of object and wavelength.

Most of the work in through wall detection is currently focused on the imaging in which researchers are working on target detection using algorithms such as back-projection [4–6] and beamforming [7, 8]. Detection of different types of target with low and high dielectric constants is a challenging task. In imaging, the presence of metal target will reflect more energy and appears bright while target having low dielectric constant will reflect less energy and appear dark that makes the detection task challenging. So, we have focused on detection of two targets having dielectric contrast in the same scene by using clutter reduction techniques.

Researchers are using various clutter removal techniques in ground penetrating radar (GPR) data but still in TWI; importance of these techniques has to be explored. Clutter reduction techniques are classified among others as statistical signal processing [9], classical filtering [10–12] and non linear signal processing based on neural networks [13, 14]. Automatic clutter reduction based on combination

using statistical and multilayer perceptrons is described in [15]. Clutter reduction based on statistical signal processing techniques such as PCA [16–18], ICA [19–23], method of FA [24–26], and SVD [27, 28] is considered in present paper to remove or minimize the clutter. All these techniques have their own advantages in image processing. For example, ICA and PCA have feature extraction property. After processing data using these techniques, SNR of images has been calculated, and results are compared.

The paper is organized in following order. Experimental setup and measurement procedure are outlined in Section 2. Section 3 deals with data preprocessing while Section 4 elaborates the principles of various clutter removal techniques which are used in this paper. Results and discussion are covered in Section 5 followed by conclusion in Section 6.

## 2. EXPERIMENTAL SETUP AND MEASUREMENT PROCEDURE

We have indigenously assembled step frequency continuous wave radar (SFCW) [29] system for scanning the wall in the frequency band of 3.95 to 5.85 GHz at 4001 points. The stepped frequency continuous wave radar has many advantages such as wider dynamic range, higher mean power, lower noise figure, and the most important one is the possibility of shaping the power spectral density. SFCW radar also provides single and multi frequencies processing, time-frequency analysis, polarimetric processing. The main advantage of SFCW radar system is its high resolution in downrange.

In this setup Rohde & Schwarz vector network analyzer (VNA) ZVB8 is used, which generates a stepped frequency waveform. A pyramidal horn antenna is used in a monostatic mode having bandwidth 1.9 GHz for transmitting and receiving signal. Circulator in the same band was used for separating the received signal from the transmitted signal. The antenna was mounted on 2D-scanning frame made of wood on which the antenna can slide along crossrange and along height. Observations were taken for 30 antenna positions in cross range direction by shifting the antenna by 5 cm at each scanning point (Figure 1). The observations have been carried out for A-scan and B-scan. A-scan is obtained by stationary measurement, transmission and collection of a signal after placing the antenna above the position of interest. The collected signal is presented as signal strength vs time delay or distance, and B-scan (or two dimensional data presentation) signal is obtained as horizontal collection from ensemble of A-scans. The horizontal axis of the two dimension image consists of crossrange (antenna position), and vertical axis is downrange (distance from the

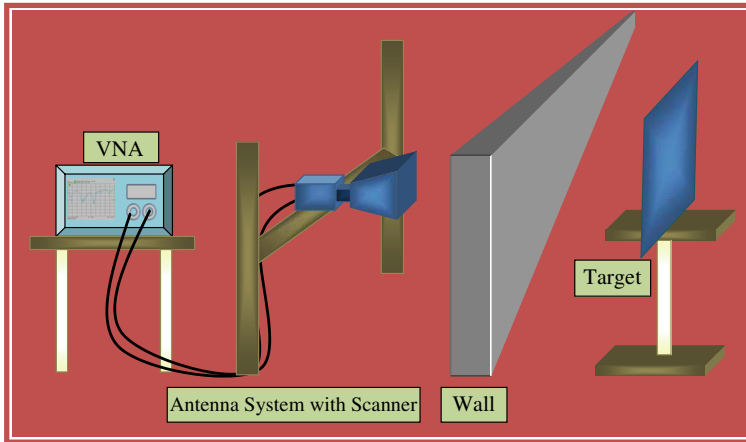


**Figure 1.** Block diagram of experimental setup for TWI.

antenna along the propagation direction of wave).

After calibrating VNA by standard two port calibration process Through Open Short Matched (TOSM), the scattering parameters  $S_{21}$  was measured at 4001 frequency points with the step size of 0.475 MHz in presence and absence of target. Data are taken in frequency domain, so it is converted to time domain by Inverse Fast Fourier Transform (IFFT) for imaging.

Plywood wall of thickness of 12 mm is used for observation. An aluminum metal plate of circular shape having diameter 58 cm and a circular Teflon plate of diameter 50 cm behind the plywood wall have been taken as a target, and both are separated in a distance of 30 cm in cross range. Wall is kept at a distance of 190 cm from antenna, and targets are kept at a distance of 30 cm from wall; therefore, total distance from antenna to target is 221.2 cm. Though the maximum room dimension in down range is not more than 5 m; the maximum unambiguous range is taken more so that the other irrelevant signals do not affect target detection.

### 3. DATA PROCESSING

#### 3.1. Calibration Using Metal Sheet

In order to identify the delay due to antenna system, calibration using metallic plate was carried out. The metallic plate (reference) is kept at a known distance, and the range profile is plotted by which delay due to antenna system is calculated. The reflection from antenna system

which was found through calibration should be subtracted to find out the exact distance between antenna system and wall.

First of all, frequency domain data collected at 4001 points are converted into time domain using Inverse Fast Fourier Transform (IFFT) given by (1)

$$s(t) = \sum_{n=0}^{N-1} S(f_n) \exp(j2\pi f_n t) \quad (1)$$

where frequency  $f_n$  varies from  $f_0$  to  $f_0 + n\Delta f$ ;  $f_0$  is the starting frequency which is 3.95 GHz;  $n$  is the number of discrete points varies from 0 to 4000;  $\Delta f$  is the frequency step size which is 0.475 GHz;  $t$  varies from 0 to  $(N - 1)/\text{BW}$  with step interval of  $1/\text{BW}$ ; BW is bandwidth of the system which is 1.9 GHz;  $S(f_n)$  is received signal in frequency domain at  $n$ th frequency point;  $s(t)$  is time domain signal.

If the reference plate is located at a known distance of  $R_{ref}$  from antenna then one way propagation delay  $t_{ref}$  is given by (2)

$$t_{ref} = \frac{R_{ref}}{c} \quad (2)$$

where  $c$  is the speed of light.

If  $t_{disp}$  is the time after which we are getting reflection from reference plate then delay due to antenna system can be calculated by (3)

$$t_{delay} = t_{disp} - t_{ref} \quad (3)$$

The corrected time domain signal that removes the phase dispersion within antenna system is given by (4)

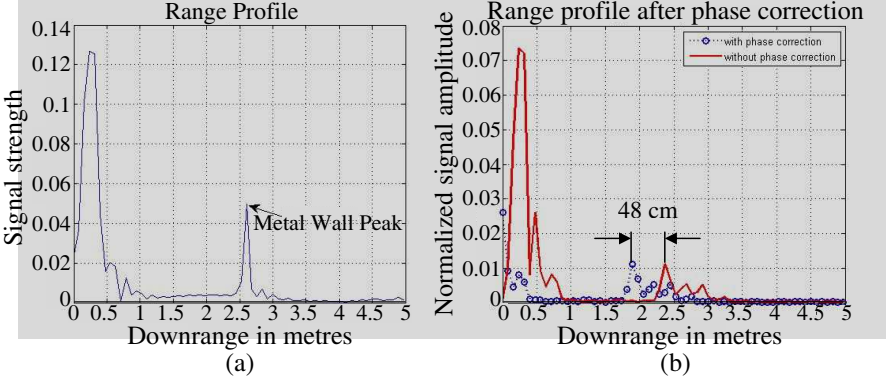
$$s(t, t_{delay}) = \sum_{n=0}^{N-1} S(f_n) \exp(j2\pi f_n (t + t_{delay})) \quad (4)$$

Figure 2(a) shows the results when the metallic plate is placed at the location of wall for calibration. In Figure 2(b), two range profiles are shown, where range profile shown in solid line (red line) is original one, and range profile shown in circled (blue color) is after phase correction. It is found that due to delay whole range profile is shifted by 48 cm.

### 3.2. Range Selection

For range selection, time domain signal must be converted into spatial domain given by (5)

$$S(z) = \sum_{n=0}^{N-1} S(f_n) \exp(j2\pi f_n t) \quad (5)$$



**Figure 2.** Range profile for calibration: (a) When metallic plate (reference) is placed at known distance, (b) after phase correction when plywood wall is placed and a Teflon target behind it.

where  $z$  is distance in downrange which can be calculated as  $z = \frac{ct}{2}$ .

Since data are collected at 4001 points, the maximum range is calculated by  $Z_{\max} = \frac{c(N-1)}{2BW}$ . In our experiment it is approximately 315 m with range resolution  $\Delta Z = \frac{c}{2N\Delta f}$ , which is 7.89 cm. Since room dimension is small, so 5 m range is considered for displaying range profile.

#### 4. CLUTTER REMOVAL TECHNIQUES

Clutter reduction is the main part in through wall imaging to accurately detect the target and remove the unwanted signals which arise due to the first reflection from the wall and other reflections due to unwanted objects. Once the signal is transmitted through the antenna, it suffers attenuation due to wall and other obstacles. Therefore, the main aim of this paper is to reduce clutter due to wall and enhance the peak due to target using signal processing techniques. Generally in signal processing terms, the techniques used for clutter reductions are called blind source or signal separation methods and concerned with the separation of a set of signals called source signals from their mixture signals, without acquaintance of any information (or with very little information) about mixing background and sources. Blind source separation is the separation of a set of signals into a set of other signals in which the regularity between the signals is minimized (decorrelation is minimized) or the regularity between the signals is maximized (statistical independence is maximized). For TWI system,

it is assumed that the scattered response is composed of superposition of responses from individual scatterers, i.e., linear model. Thus, mainly three components are assumed. One is measurement noise; second is clutter; third is reflection from desired target. All the unwanted contributions like antenna cross talk, wall reflection and multiple reflections are considered as clutter. Thus, using clutter reduction techniques, source signal can be decomposed into desired target and clutter.

Some important clutter removal techniques which are generally used in GPR data have been applied and analyzed in the present paper [31]. Brief descriptions of these techniques are given in following subsections.

#### 4.1. Singular Value Decomposition (SVD)

SVD has many applications in signal processing and image processing that can be used for many purposes such as noise reduction, information retrieval, compression, and patterns detection [27, 28]. The main use of SVD is to split the data matrix into complementary subspaces called signal and noise subspaces in order to increase SNR which is useful for clutter reduction.

For clutter reduction using SVD, B-scan data are represented by a rectangular matrix  $X_{ij}$ , whose dimension is  $M \times N$ , ( $i = 1, 2, \dots, M; j = 1, 2, \dots, N$ ). Here  $i$  denotes the time or distance index, and  $j$  denotes the antenna position index. The number of discrete distance points is greater than the antenna index; therefore  $M \geq N$  will be assumed. SVD of  $X$  is given by (6)

$$X = USV^T \quad (6)$$

where  $U$  and  $V$  are  $(M \times M)$  and  $(N \times N)$  unitary matrices respectively and  $S = \text{diag}(\sigma_1, \sigma_2, \dots, \sigma_r)$  with  $\sigma_1 \geq \sigma_2 \geq \dots \geq \sigma_r \geq 0$ . The columns of  $U$  and  $V$  are called the left and right singular vectors respectively. Basically  $U$  and  $V$  are the eigenvectors of  $\{XX^T\}$  and  $\{X^T X\}$ . For ( $r = N < M$ ), the SVD is given by (7)–(9)

$$\begin{aligned} X = \sigma_1 \begin{pmatrix} \vdots \\ u_1 \\ \vdots \end{pmatrix} (\cdots v_1^T \cdots) + \sigma_2 \begin{pmatrix} \vdots \\ u_2 \\ \vdots \end{pmatrix} (\cdots v_2^T \cdots) + \cdots \\ + \sigma_N \begin{pmatrix} \vdots \\ u_N \\ \vdots \end{pmatrix} (\cdots v_N^T \cdots) \end{aligned} \quad (7)$$

$$X = \sum_{i=1}^N \sigma_i u_i v_i^T \quad (8)$$

$$X = M_1 + M_2 + M_3 + \dots + M_N \quad (9)$$

where  $M_i$  are matrices of the same dimensions of  $X$  and called as modes or  $i$ th eigenimage of  $X$ .  $X$  can be decomposed into two subspace, signal and clutter respectively.

$$X = X_{signal} + X_{clutter} = \sum_{i=1}^k \sigma_i u_i v_i^T + \sum_{i=k+1}^N \sigma_i u_i v_i^T \quad (10)$$

After applying SVD to our experimental data and analyzing all the eigen images obtained using (9), we found that first eigen image  $M_1$  provides the clutter information; second eigen image  $M_2$  provides the target information; rest eigen images represent the noise. B-scan data  $X$  can be split into three parts.

$$X = M_t + M_c + M_n \quad (11)$$

where  $M_t$ ,  $M_c$  and  $M_n$  are the target, background (i.e., clutter) and noise images respectively. Clutter can be estimated by (12), target by (13) and noise image by (14)

$$M_c = M_1 = \sigma_1 \times u_1 \times v_1^T \quad (12)$$

$$M_t = M_2 = \sigma_2 \times u_2 \times v_2^T \quad (13)$$

$$M_n = \sum_{i=3}^N \sigma_i u_i v_i^T \quad (14)$$

## 4.2. Factor Analysis

Factor analysis is a general term for a family of statistical techniques. It uses correlations between observed variables to estimate common factors. It makes use of second order statistics to extract signal so that signal to noise ratio can be increased. Also, factor analysis is concerned with the dimensional (number of variables) reduction of a set of observed data in terms of a small number of latent factors [24–26]. The main application of Factor Analysis is to reduce data variables and to classify them.

Basically Factor Analysis extracts the set of factors from data set using correlation. Generally these factors are orthogonal and are ordered according to the proportion of the variance of the original data.

Therefore in general, only a (small) subset of factors is considered as relevant, and the remaining factors are considered as either irrelevant or nonexistent. The observed variables can be written as the linear combinations of the factors plus error terms.

For clutter reduction, B-scan data are represented by a rectangular matrix  $X_{ij}$ , whose dimension is  $M \times N$ , ( $i = 1, 2, \dots, M; j = 1, 2, \dots, N$ ). Here  $i$  denotes the time or distance index, and  $j$  denotes the antenna position index. The observed variables are modeled as linear combinations of the factors plus error terms.

$$x_i = \sum_{j=1}^N a_{ij}s_j + e_i \quad (15)$$

In matrix notation it can be written by (16)

$$X = AS + E \quad (16)$$

where  $X$  is the matrix consisting the  $M$  A-scans in each row with  $N$  time samples;  $S$  is the  $N \times K$  matrix of factor scores (latent variables);  $A$  is the  $M \times N$  matrix of factor loading;  $E$  is a matrix of error terms. The Factor Analysis can be modeled in terms of variances and covariances given by (17)

$$\Sigma = A\Phi A^T + \Psi \quad (17)$$

where  $\Sigma$  is the  $M \times M$  population covariance matrix of the observed variables;  $\Phi$  is the  $N \times N$  covariance matrix of the factors;  $\Psi$  is the  $M \times M$  residual covariance matrix.

The primary assumption is that factors are uncorrelated, which implies covariance matrix should be identity matrix i.e.,  $\Phi = I$ , and the  $M$ -dimensional  $e$  is distributed according to  $N(0, \Psi)$ , where  $\Psi$  is diagonal matrix. The assumption of diagonality of  $\Psi$  implies that the observed variables are conditionally independent (given the factors). The distribution of observed variable  $x$  must have zero mean and covariance  $\Sigma$ .

Factor Analysis finds optimal  $A$  and  $\Psi$  which best describe the covariance structure of  $x$ . The best model of  $A$  and  $\Psi$  can be found using Expectation Maximization (EM) algorithm [32]. The EM procedure is a two step iterative procedure for maximizing the log likelihood. A brief explanation of generalized EM algorithm for maximum likelihood method is discussed in this paper. Detail explanation of EM algorithm for maximum likelihood Factor Analysis is given in [33].

In Expectation step, it calculates the expected value of log likelihood function with respect to unknown variable  $z$  given by Eq. (18)

$$Q\left(Y \mid Y^{(T)}\right) = E_{z|x, Y^{(T)}} [\log L(Y|X, Z)] \quad (18)$$

where  $Y$  is the unknown parameter to be estimated under the conditional distribution of  $Z$  when  $X$  is given;  $L(Y|X, Z)$  is the likelihood function.

Maximization step finds the optimal parameter values that maximize the expectation which is computed in expectation step given by (19)

$$Y^{(T+1)} = \arg \max_Y \left\{ Q\left(Y \mid Y^{(T)}\right) \right\} \quad (19)$$

Apply these two steps iteratively until a converged solution for  $Y$  is obtained. After applying FA on experimental data, we found that it splits data matrix  $X$  into factor score matrix  $S$  and factor loading matrix  $A$  given by (16). Target can be extracted by selecting the factor score and factor loadings components which carry the target information and given by (20). Generally the second column of  $A$  and  $S$  gives the information of target, and first column gives the information of clutter.

$$X_{target} = A_2^T S_2 \quad (20)$$

### 4.3. Principal Component Analysis (PCA)

PCA isolates the components on the basis of high correlation due to large size of B-scan matrix. If highly correlated components are present then the accuracy of algorithm will increase. Remaining uncorrelated components can be removed easily. PCA can be used in many applications, such as signal processing, data compressing, data visualization, image analysis and pattern recognition. PCA can be used for noise reduction in images by using the concept of dimensionality reduction [16, 17].

For clutter reduction using PCA, B-scan data are represented by a rectangular matrix  $X_{ij}$ , whose dimension is  $M \times N$  ( $i = 1, 2, \dots, M$ ;  $j = 1, 2, \dots, N$ ). Here  $i$  denotes the time or distance index, and  $j$  denotes the antenna position index.  $N$  principal components of data matrix  $X$  can be given by (21)

$$Y = A^T X \quad (21)$$

where  $X = [x_1, x_2, x_3, \dots, x_n]^T$  is the zero-mean input vector;  $Y = [y_1, y_2, y_3, \dots, y_n]^T$  is the output vector called the vector of principal components (PCs);  $A$  is an  $M \times N$  matrix that transforms  $X$  into

$Y$ . The purpose of PCA is to derive a relatively small number of decorrelated linear combination (principal component) of a set of random zero-mean variables while retaining as much of the information from the original variables as possible. Therefore, PCA expresses input data variables into smaller number of decorrelated linear combination of a set of zero mean random variables, while retaining as much of the information from the original variables as possible. The basic idea in PCA is to find the rows of the  $y_1^T, y_2^T, y_3^T \dots, y_n^T$ . PCA assumes that  $A$  is an orthonormal matrix ( $A_i^T \cdot A_j = \delta_{ij}$ ) such that the covariance matrix of  $Y$ ; ( $C_y$ ) is diagonalized.

$A$  can be computed using covariance matrix. Let  $X$  be the data matrix after normalization and subtracting the mean. Then covariance matrix  $C_x$  of  $X$  is given by (22)

$$C_x = \frac{1}{N} X X^T \quad (22)$$

The eigenvector and eigenvalue matrices of  $C_x$  are  $\Phi$  and  $\Lambda$  respectively and can be computed by (23)

$$C_x \Phi = \Phi \Lambda \quad (23)$$

where  $\Lambda = \text{diag}(\lambda_1, \lambda_2, \lambda_3, \dots, \lambda_N)$  and  $\lambda_1, \lambda_2, \lambda_3, \dots, \lambda_N$  are the eigen values. After arranging eigen values in the decreasing order,  $\lambda_1 \geq \lambda_2 \geq \lambda_3 \geq \dots \geq \lambda_N$  the matrix of  $N$  leading eigen vectors  $A$  is given by (24)

$$A = [\Phi_1, \Phi_2, \Phi_3, \dots, \Phi_N] \quad (24)$$

Principal component matrix  $S$  can be given by (25)

$$S = A^T X \quad (25)$$

It infers that PCA can be used as given in Eq. (25) for detection of the targets or objects behind the walls. This can be done by selecting some components that mainly carry target information, say  $A_p$ , and rest components represent the clutter. The reconstructed clutter-free signal space can be extracted from the original B-scan matrix containing target and clutter information. After calculating principal components, target can be extracted by second column of  $A$  and  $S$ . Generally, first eigen image represents the clutter, and second eigen image represents the target. It means that second column of transformation matrix  $A$  i.e.,  $A_2$  and principal component matrix  $S$  i.e.,  $S_2$  represents the target that is given by (26).

$$X_{target} = A_2^T S_2 \quad (26)$$

#### 4.4. Independent Component Analysis (ICA)

ICA is used to solve blind source separation problem. ICA divides data into statistically independent components while other techniques such as PCA or FA represents data into uncorrelated components. Therefore, PCA or FA cannot separate signals efficiently because uncorrelatedness is not enough. Statistical independence is necessary which takes into consideration higher order moments which are stronger statistical properties than decorrelation. Therefore, ICA is widely used in many applications such as feature extraction and noise reduction from the images, finding hidden factors from financial data and mostly used in telecommunications for separating the original source signal from interfering signals [18–22]. In ICA model, it is assumed that the observed data  $X$  have been generated from source data  $S$  through a linear process  $X = AS$ , where both the sources  $S$  and mixing matrix  $A$  are unknown. ICA algorithms are able to estimate both the sources  $S$  and mixing matrix  $A$  from the observed data  $X$  with very few assumptions [16–21].

For clutter reduction using ICA, B-scan data are represented by a rectangular matrix  $X_{ij}$ , whose dimension is  $M \times N$  ( $i = 1, 2, \dots, M; j = 1, 2, \dots, N$ ). Here  $i$  denotes the time index, and  $j$  denotes the antenna position index.

ICA assumes that every  $x_i$  is a linear combination of each  $s_j$  given by (27)

$$x_i = \sum_{j=1}^N a_{ij} s_j \quad (27)$$

$j = 1, 2, 3, \dots, N$  or in the matrix notation

$$X = AS \quad (28)$$

Here  $A$  is an  $M \times N$  basis transformation or mixing matrix, and  $S$  is the matrix holding the  $N$  independent source signals in rows of  $N$  samples. ICA of matrix  $X$  can be obtained by finding a full rank separating matrix  $W$  such that output signal matrix can be defined by  $Y = WX$ . The estimation of source signal can be given by (29)

$$\hat{s}_j = y_j = \sum_{i=1}^N w_{ji} x_i \quad (29)$$

$j = 1, 2, 3, \dots, N$  or in the matrix notation

$$\hat{S} = Y = WX \quad (30)$$

where  $W$  is a  $N \times M$  matrix which makes the outputs  $\widehat{S}$  from the linear transformation of the dependent sensor signals  $x$  as independent as possible.

Formulation of ICA can be done in two steps. First one is to formulate a contrast function  $G(y)$  that estimates the level of statistical independence between the components of  $y$ , and second one is the optimization of contrast function that enables the calculation of independent components. Contrast function estimates the level of statistical independence between the components of  $y$  i.e., optimization of contrast function provide the independent components. To apply ICA, some preprocessing is needed. The most basic preprocessing is centering in which the mean is subtracted from each range profile in B-scan matrix  $X$ . Second preprocessing is whitening in which observed vector  $X$  is transformed into new vector  $\tilde{X}$  which is white i.e., its components are un-correlated, and their variance is equal to unity.

Here we have used the FASTICA [23] algorithm which is fixed point iteration based algorithm to calculate the separating matrix  $W$  by finding a maximum of non Gaussianity of  $W^T \tilde{X}$ . After computing the separating matrix  $W$ , mixing matrix  $A$  can be computed by taking inverse of it i.e.,  $A = W^{-1}$ . Since mixing matrix is known, corresponding independent component  $S$  matrix can be calculated using (28).

After applying ICA on experimental data, we are able to get the number of independent components as much the number of sources or A-scans. By considering each row of independent component matrix  $S$  and column of mixing matrix  $A$ , images have been generated using (28) and observed. Image that contains target information can be chosen, and remaining is discarded.

$$X_{target} = A_{target} S_{target} \quad (31)$$

## 5. RESULTS AND DISCUSSION

Clutter reduction techniques discussed in above sections are applied to the experimental data, and the images have been compared on the basis of signal to noise ratio (SNR). SNR can be given as the ratio of average energy of the image matrix after clutter reduction to the average energy of clutter plus noise matrix. So in the denominator term, we will get clutter plus noise term by subtracting it from raw B-scan image. The final image after applying clutter reduction is supposed to have only information about the target, but actually it is not and contains good amount of background noise that we have obtained after applying different clutter reduction techniques.

Therefore, in the numerator term, we have not taken average energy of image giving target information because this contributes more to the numerator term of SNR and difficult to compare different clutter reduction techniques in this paper. Therefore, we have considered the peak signal to noise ratio (PSNR) [34] in which numerator term of SNR is taken as the peak value of normalize image matrix. It infers that PSNR may be used as a first hand indicator to compare the results of various clutter reduction techniques. PSNR can be calculated using (32) and (33).

$$\text{PSNR (dB)} = 10 \log \{1/MSE\} \quad (32)$$

$$MSE = \frac{1}{M \times N} \sum_{i=1}^N \sum_{j=1}^M \{g(i, j) - f(i, j)\}^2 \quad (33)$$

where  $g(i, j)$  is our original B-scan image;  $f(i, j)$  is the reconstructed image after clutter reduction;  $MSE$  is mean square error;  $M$  and  $N$  are dimensions of image.

Results after applying clutter reduction techniques are shown in Figure 3 that includes A-scan (range profile) and B-scan images. In A-scan, solid line shows original target with wall, while dashed line represents target signal estimated using clutter removal techniques. B-scan images are obtained after clutter reduction.

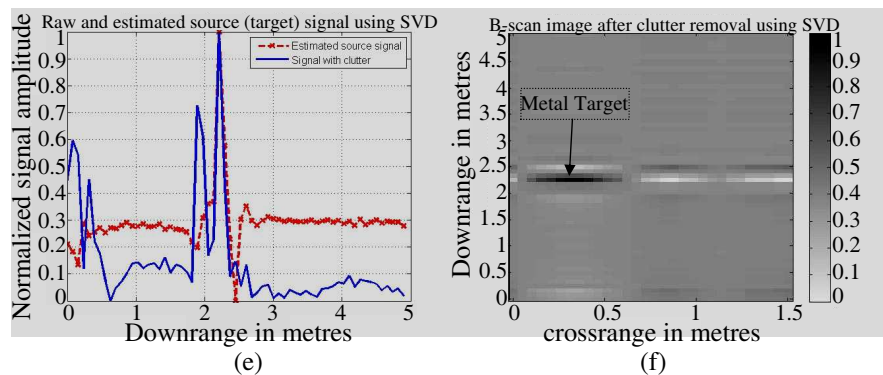
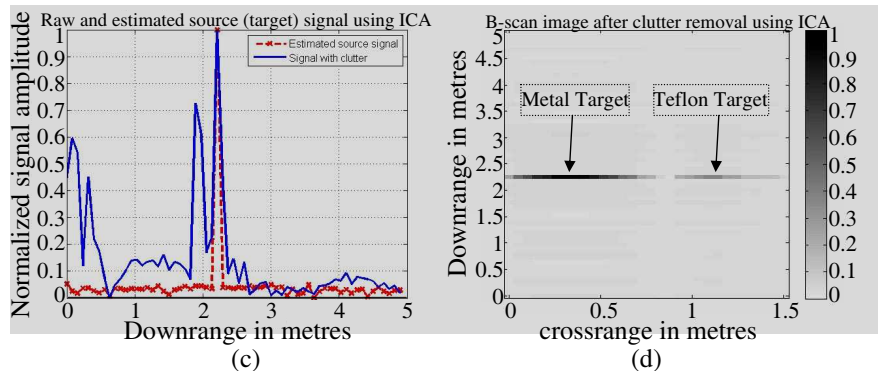
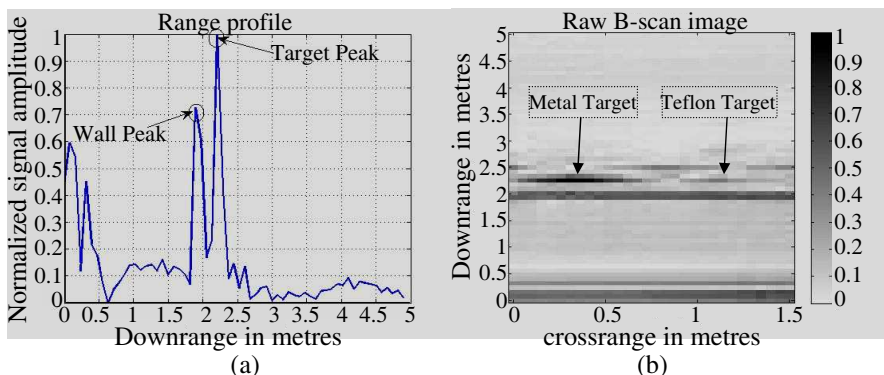
Figure 3(a) shows the range profile of raw data (without clutter reduction) in which target peak at 221 cm and wall peak at 190 cm are observed, and B-scan image is shown in Figure 3(b) in which both metal and Teflon targets are displayed, but Teflon target is suppressed because of clutter.

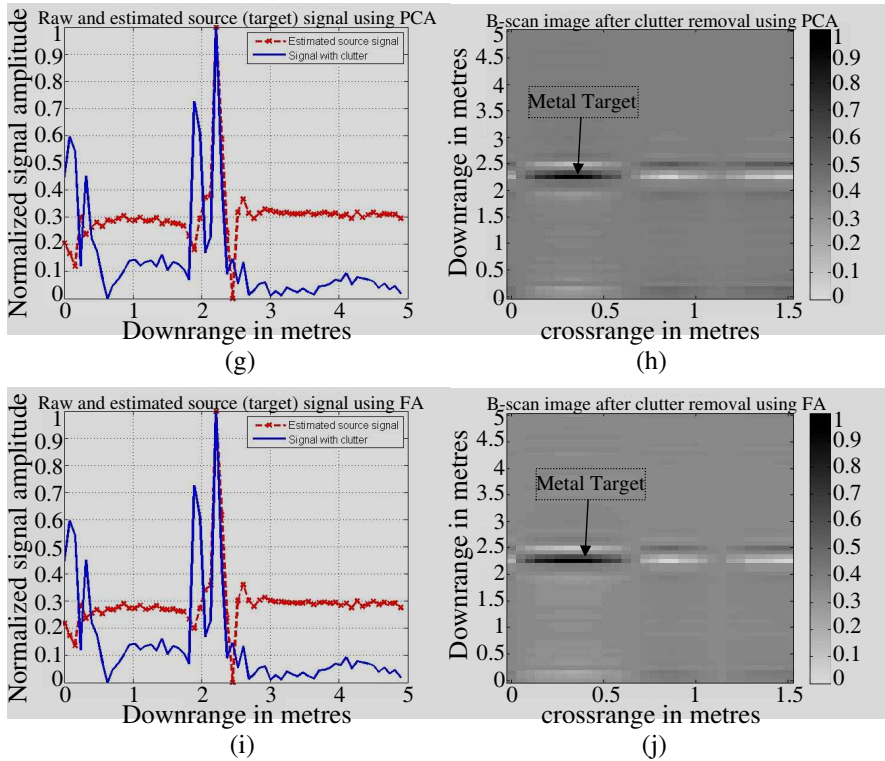
Range profiles are observed for both targets. It is found that only metal target peak is visible, while Teflon target is not detected clearly in SVD, FA and PCA techniques whereas in ICA it is observed. It may be due to the reason that the reflected signal strength with metal target will be high in comparison to Teflon target. Figure 3(c) shows the range profile of the metal target signal with ICA. The signal after ICA is shown in dashed line and compared with original signal containing wall and target reflections peak shown in solid line. From this figure, we can observe that only target peak is enhanced, and noise floor is very low. Figure 3(d) shows the B-scan image after clutter reduction using ICA in which both targets are clearly visible at the distance about 221 cm in down range. This image has very low background noise (0.0 to 0.2 normalized values).

Figure 3(e) shows the range profile of metal target with SVD clutter reduction technique. In this figure, it is observed that target

peak is enhanced; clutter is suppressed in one hand, and in the other hand noise floor is also increased. This can be more visualized in B-scan image (Figure 3(f)), where metal target is clearly visible, but second target (Teflon) is mixed with clutter. In this figure, noise level is also high (in between 0.3 to 0.4 normalized values).

Figures 3(g) and 3(h) show A-scan and B-scan images after PCA





**Figure 3.** (a) Range profile of raw data (without clutter reduction), (b) B-scan of raw data (without clutter reduction), (c) Range profile with and without clutter reduction using ICA, (d) B-scan after using ICA, (e) Range profile with and without clutter reduction using SVD, (f) B-scan after using SVD, (g) Range profile with and without clutter reduction using PCA, (h) B-scan after using PCA, (i) Range profile with and without clutter reduction using FA, (j) B-scan after using FA.

clutter reduction technique, whereas Figures 3(i) and 3(j) show A-scan and B-scan images after FA clutter reduction techniques. In all these figures i.e., 3(h) and 3(j), it is clearly observed that the detection of metal target is enhanced, while background noise is not so much suppressed by these techniques and secondly, it is difficult to detect the second low dielectric target i.e., Teflon. If we compare the results of various clutter reduction techniques (i.e., Figures 3(c) to 3(j)), it is clearly observed that ICA based technique outperforms in comparison to other techniques for extracting target feature of low dielectric material from the raw clutter data.

**Table 1.** Performance of clutter reduction algorithms on basis of PSNR.

S. No.	Clutter reduction Algorithm	PSNR (dB)	Results
1.	Independent Component Analysis (ICA)	36.25	Both metal and Teflon target detected
2.	Factor Analysis (FA)	26	Only metal target detected
3.	Singular Value Decomposition (SVD)	23.6	Only metal target detected
4.	Principal Component Analysis (PCA)	23.42	Only metal target detected

The performance of these clutter reduction techniques is compared using the PSNR of B-scan images. PSNR of the images is computed by using (32) and (33). Table 1 shows comparison of clutter reduction techniques, and it is clearly observed that ICA has better PSNR in comparison to other three techniques. Another observable point is that we are unable to detect the Teflon target using PCA, SVD and Factor Analysis. Only ICA is capable of extracting that target as we can see from Figure 3(d).

## 6. CONCLUSION

A TWI system in UWB range has been assembled, and various data for A-scan and B-scan have been collected. The focus of present paper is to explore the possibility of application of various existing clutter removal techniques for TWI data and also to check the possibility of detection of low dielectric target. For this purpose, different clutter removal algorithms have been implemented and compared. ICA based technique gives a better result than other clutter removal techniques like SVD, PCA and FA. PSNR for B-scan image is quite high in case of ICA compared to other techniques. It is also observed that ICA based clutter removal technique have a better potential to detect low dielectric constant target like Teflon behind the plywood wall. In future, analysis will be carried out for different walls like brick wall, asbestos wall etc. All the clutter reduction techniques which are considered in this paper are based on the assumption of linear mixture of signals. Thus, non linear model may be studied in future as it is more realistic.

**REFERENCES**

1. Baranoski, E. J., "Through-wall imaging: Historical perspective and future directions," *J. Franklin Inst.*, Vol. 345, 556–569, Jan. 2008.
2. Farwell, M., J. Ross, R. Luttrell, D. Cohen, W. Chin, and T. Dogaru, "Sense through the wall system development and design considerations," *J. Franklin Inst.*, Vol. 345, 570–591, Jan. 2008.
3. Dehmollaian, M., M. Thiel, and K. Sarabandi, "Through-the-wall imaging using differential SAR," *IEEE Trans. Geosci. Remote Sens.*, Vol. 47, No. 5, 1289–1296, May 2009.
4. Yegulalp, A. F., "Fast backprojection algorithm radar for synthetic aperture," The Record of the 1999 IEEE Radar Conference, 60–65, Waltham, MA, USA, Apr. 1999,
5. Cui, G., L. Kong, and J. Yang, "A back-projection algorithm to stepped-frequency synthetic aperture through-the-wall radar imaging," *IEEE 1st Asian and Pacific Conference on Synthetic Aperture Radar, APSAR 2007*, 123–126, 2007.
6. Lundgren, W., U. Majumder, M. Backues, K. Barnes, and J. Steed, "Implementing SAR image processing using backprojection on the cell broadband engine," *IEEE Conference on Radar*, 1–6, May 2008.
7. Ahmad, F., M. G. Amin, S. A. Kassam, and G. J. Frazer, "A wideband synthetic aperture beamformer for through-the-wall imaging," *IEEE International Symposium on Phased Array Systems and Technology*, 187–192, Oct. 2003.
8. Xu, X. and R. M. Narayanan, "Enhanced resolution in SAR/ISAR imaging using iterative sidelobe apodization," *IEEE Trans. Image Processing*, Vol. 14, No. 4, 537–547, Apr. 2005.
9. Xu, X., E. L. Miller, C. M. Rappaport, and G. D. Sower, "Statistical method to detect subsurface objects using array ground-penetrating radar data," *IEEE Trans. Geosci. Remote Sensing*, Vol. 40, 963–976, Apr. 2002.
10. Merwe, A. V. and I. J. Gupta, "A novel signal processing technique for clutter reduction in GPR measurements of small, shallow land mines," *IEEE Trans. Geosci. Remote Sensing*, Vol. 38, 2627–2637, Nov. 2000.
11. Zoubir, A. M., I. J. Chant, C. L. Brown, B. Barkat, and C. Abeynayake, "Signal processing techniques for landmine detection using impulse ground penetrating radar," *IEEE Sensors J.*, Vol. 2, No. 1, 41–51, Feb. 2002.

12. Kempen, V. L. and H. Sahli, "Signal processing techniques for clutter parameters estimation and clutter removal in GPR data for landmine detection," *Statistical Signal Processing, 2001 Proceedings of the 11th IEEE Signal Processing Workshop*, 158–161, May 2001.
13. Vicen-Bueno, R., R. Carrasco-Ivarez, M. Rosa-Zurera, and J. C. Nieto-Borge, "Sea clutter reduction and target enhancement by neural networks in a marine radar system," *Sensors*, Vol. 9, 1913–1936, 2009.
14. Chan, L. A., N. M. Nasrabadi, and D. Torrieri, "Eigenspace transformation for automatic clutter rejection," *Optical Engineering*, Vol. 40, No. 4, 564–573, Apr. 2001.
15. Xie, N., H. Leung, and H. Chang, "A multiple-model prediction approach for sea clutter modeling," *IEEE Trans. Geosci. Remote Sensing*, Vol. 41, 1491–1502, Jun. 2003.
16. Yu, C. Q., X. S. Guo, A. Zhang, and X. J. Pan, "An improvement algorithm of principal component analysis," *International Conference on Electronic Measurement and Instruments*, 2529–2534, Jul. 2007.
17. Diamantaras, K. I., "PCA neural models and blind signal separation," *International Joint Conference on Neural Networks*, Vol. 4, 2997–3002, Jul. 2001.
18. Abujarad, F. and A. Omar, "GPR data processing using the component-separation methods PCA and ICA," *IEEE International Workshop on Imaging Systems and Techniques*, 60–64, Apr. 2006.
19. Karlsen, B., J. Larsen, H. B. D. Sorensen, and K. B. Jakobsen, "Comparison of PCA and ICA based clutter reduction in GPR systems for anti-personal land-mine detection," *Proceedings of the 11th IEEE Signal Processing Workshop on Statistical Signal Processing*, 146–149, Aug. 2001.
20. Comon, P., "Independent component analysis, a new concept," *Signal Processing*, Vol. 36, 287–314, Apr. 1994.
21. Baloch, S. S. H., H. Krim, and M. G. Genton, "Robust independent component analysis," *13th IEEE Workshop on Statistical Signal Processing*, 61–64, Jul. 2005.
22. Hyvarinen, A., J. Karhunen, and E. Oja, *Independent Component Analysis*, John Wiley and Sons, USA, 2001.
23. Hyvarinen, A., "Fast and robust fixed-point algorithms for independent component analysis," *IEEE Trans. Neural Net.*, Vol. 10, No. 3, 626–634, 1999.

24. Chen, C. H. and W. Zhenhai, "ICA and factor analysis application in seismic profiling," *IEEE International Conference on Geoscience and Remote Sensing Symposium*, 1560–1563, Aug. 2006.
25. Wu, N. and J. Zhang, "Factor analysis based anomaly detection," *Information Assurance Workshop, 2003, IEEE Systems, Man and Cybernetics Society*, 108–115, Jun. 2003.
26. Hong, S., "Warped image factor analysis," *1st IEEE International Workshop on Computational Advances in Multi-sensor Adaptive Processing*, 121–124, Dec. 2005.
27. Abujarad, F., A. Jostingmeier, and A. S. Omar, "Clutter removal for landmine using different signal processing techniques," *Proceedings of the Tenth IEEE International Conference on Ground Penetrating Radar, GPR 2004*, 697–700, Jun. 2004.
28. Wall, M. E., A. Rechtsteiner, and L. M. Rocha, "Singular value decomposition and principal component analysis," *A Practical Approach to Microarray Data Analysis*, Chapter 5, 91–109, Boston, MA, USA, 2003.
29. Chandra, R., A. N. Gaikwad, D. Singh, and M. J. Nigam, "An approach to remove the clutter and detect the target for ultra-wideband through-wall imaging," *Journal of Geophysics and Engineering*, Vol. 5, 412–419, Oct. 2008.
30. Cois Cardoso, J., "Blind signal separation: Statistical principles," *IEEE Proc.*, Vol. 86, No. 10, 2009–2025, Oct. 1998.
31. Liu, J. X., B. Zhang, and R. B. Wu, "GPR ground bounce removal methods based on blind source separation," *PIERS Online*, Vol. 2, No. 3, 256–259, 2006.
32. Saul, L. K. and M. G. Rahim, "Maximum likelihood and minimum classification error factor analysis for automatic speech recognition," *IEEE Trans. Speech Audio Process.*, Vol. 8, No. 2, 115–125, Mar. 2000.
33. Rubin, D. and D. Thayer, "EM algorithms for factor analysis," *Psychometrika*, Vol. 47, No. 1, 69–76, Mar. 1982.
34. Wei, G. W., "Generalized Perona-Malik equation for Image restoration," *IEEE Signal Proc. Letters*, Vol. 6, No. 7, 165–167, Jul. 1999.